

Investigating spatial variability of vertical water fluxes through the streambed in distinctive stream morphologies using temperature and head data

Liping Wang¹ · Weiwei Jiang² · Jinxi Song^{1,3} · Xinyi Dou¹ · Hongtao Guo⁴ · Shaofeng Xu¹ · Guotao Zhang¹ · Ming Wen¹ · Yongqing Long¹ · Qi Li¹

Received: 22 May 2016 / Accepted: 6 January 2017 / Published online: 3 February 2017
© Springer-Verlag Berlin Heidelberg 2017

Abstract Investigating the interaction of groundwater and surface water is key to understanding the hyporheic processes. The vertical water fluxes through a streambed were determined using Darcian flux calculations and vertical sediment temperature profiles to assess the pattern and magnitude of groundwater/surface-water interaction in Beiluo River, China. Field measurements were taken in January 2015 at three different stream morphologies including a meander bend, an anabranching channel and a straight stream channel. Despite the differences of flux direction and magnitude, flux directions based on vertical temperature profiles are in good agreement with results from Darcian flux calculations at the anabranching channel, and the Kruskal-Wallis tests show no significant differences between the estimated upward fluxes based on the two methods at each site. Also, the upward fluxes based on the two methods show similar spatial distributions on the streambed, indicating (1) that higher water fluxes at the meander bend occur from the center of the channel towards the erosional bank, (2) that water fluxes at the anabranching channel are higher near the erosional bank and in the center of the channel, and (3) that in the straight channel, higher water

fluxes appear from the center of the channel towards the depositional bank. It is noted that higher fluxes generally occur at certain locations with higher streambed vertical hydraulic conductivity (K_v) or where a higher vertical hydraulic gradient is observed. Moreover, differences of grain size, induced by stream morphology and contrasting erosional and depositional conditions, have significant effects on streambed K_v and water fluxes.

Keywords Geomorphology · Groundwater/surface-water interaction · Darcian flux calculations · Vertical temperature profiles · Streambed grain size

Introduction

The transition zone between groundwater and surface-water bodies where groundwater and surface water are actively mixed and exchanged is called the hyporheic zone (Brunke and Gonser 1997; Winter 1998; Smith 2005; Hester and Gooseff 2010). The interaction between groundwater and surface water in the hyporheic zone has fairly profound influences on hydrological (Winter 1998; Constantz et al. 2002; Bencala et al. 2011), biological (Malard et al. 2002; Bruno et al. 2009; Gariglio et al. 2013), and chemical (Winter 1998; Kennedy et al. 2009; Binley et al. 2013) processes. Especially, understanding their interaction is quite critical for investigating transformations of nutrients (Brunke and Gonser 1997), habitat quality (Malcolm et al. 2008), and the fate and transport of contaminants between streams and groundwater (Conant 2004; Chapman et al. 2007; Lewandowski et al. 2011). The interaction between groundwater and surface water in the hyporheic zone can be delineated by vertical water fluxes through the streambed (Essaid et al. 2008; Anibas et al. 2011; Hyun et al. 2011; Vandersteen et al. 2015). However,

✉ Jinxi Song
jinxisong@nwu.edu.cn

¹ College of Urban and Environmental Sciences, Northwest University, Xi'an 710027, China

² College of Water Sciences, Beijing Normal University, Beijing 100875, China

³ State Key Laboratory of Soil Erosion and Dryland Farming on the Loess Plateau, Institute of Soil and Water Conservation, CAS & MWR, Yangling 712100, China

⁴ Chongqing Academy of Environmental Science, Chongqing 401147, China

the exchange of water through the streambed is a dynamic process; the flux direction and magnitude can change throughout space and time (Rau et al. 2010), which make delineating and characterizing vertical water fluxes through the streambed extremely difficult (Kalbus et al. 2006).

The heterogeneous distribution of water fluxes through the streambed can be attributed to several factors, including streambed hydraulic conductivity (Chen et al. 2009; Hyun et al. 2011), heterogeneity of streambed sediments (Conant 2004) and hydrogeology (Schornberg et al. 2010), streambed topography (Savant et al. 1987; Harvey and Bencala 1993; Frei et al. 2010), geomorphologic features at different spatial scales (Kasahara and Wondzell 2003; Cardenas et al. 2004), and hydrologic conditions in both the stream and the groundwater (Bartsch et al. 2014). Streambed vertical hydraulic conductivity is a pivotal hydrologic parameter controlling vertical water fluxes. Due to higher streambed K_v near the bank zones, higher fluxes are generally observed near the bank zones than in the center of the river (Anibas et al. 2011), but the exchange flows at the sides of the river are more variable than near the center (Storey et al. 2003). Streambed attributes in the meander bend are more variable than in the straight channel because of the more dynamic environment of the meander bends, and high K_v values occur at the erosional outer bend and near the middle of the channel (Sebok et al. 2015). The difference of streambed attributes and vertical hydraulic conductivity between the meander bend and the straight channel may lead to different spatial distribution of vertical water fluxes. Bed topography and stream sinuosity can also result in downward and upward flow paths at small (<100 m) scales (Vaux 1968; Savant et al. 1987).

There are a number of methods available to estimate vertical water fluxes (Kalbus et al. 2006). Choosing the proper method to quantify vertical water fluxes remains difficult as each of these methods has their merits and drawbacks. Seepage meters are considered cost-effective apparatuses for the quantification of water fluxes; however, seepage meters failed to detect measurable groundwater seepage while Darcian flux calculations detected groundwater seepage into the stream (Cey et al. 1998). Differential discharge gauging, stream tracer experiments and the use of numerical modeling measure spatial-averaged fluxes at the reach scale (Becker et al. 2004; Fleckenstein et al. 2004); however, the variability of local water flux into or out of the stream has significant implications for physical, chemical, and biological processes in the hyporheic zone. Remote sensing results have been more qualitative than quantitative (Loheide and Gorlick 2006). Another two common methods are Darcian flux calculations and vertical temperature profiles. Darcian flux calculations are based on streambed measurements of a vertical hydraulic head gradient (VHG) and a vertical hydraulic conductivity (K_v) to quantify vertical streambed water fluxes (Freeze and Cherry 1979). Field techniques can provide reliable estimates of K_v

(Chen 2004; Chen et al. 2009) and vertical hydraulic gradient (Chen et al. 2009; Sebok et al. 2015). Darcian flux calculations have been used in a number of field studies for addressing the interaction between groundwater and surface water (Conant 2004; Chen et al. 2009; Kennedy et al. 2010). Vertical streambed temperature profiles can be a good indicator of the Darcian flux, indicating qualitatively streambed flux direction (gaining or losing; Anibas et al. 2011), and quantifying the magnitude of upward water fluxes with steady-state analytical solutions (Suzuki 1960; Bredehoeft and Papaopulos 1965; Stallman 1965). Vertical temperature profiles have been used for estimating water fluxes on tens of meters (Taniguchi et al. 1999; Anibas et al. 2009) or centimeter scales (Hyun et al. 2011), and their spatial and temporal variability (Schmidt et al. 2007; Anibas et al. 2011; Gariglio et al. 2013). Vertical temperature profiles can be determined by temperature probes located at certain depths of streambed. The use of temperature profiles is very simple and of advantage for providing a snapshot of water fluxes in the streambed based on the assumption of the steady state of vertical temperature distributions (Anibas et al. 2009). Despite their advantages, however, using Darcian flux calculations and vertical streambed temperature profiles to estimate vertical streambed water fluxes also have distinct limitations and can only show vertical streambed water fluxes at a specific spatial or temporal scale (Kalbus et al. 2006). Darcian flux calculations are limited by the practical difficulties in estimating the hydraulic conductivity (Calver 2001). Flux estimates based on temperature profiles in the streambed may introduce errors if the assumption of steady-state or vertical flow has been violated (Schmidt et al. 2007; Anibas et al. 2009). Therefore, due to the limitations and uncertainties of a single method, it will be beneficial to combine the multiple methods to reliably estimate vertical streambed water fluxes (Kalbus et al. 2006). There are an increasing number of studies that have combined temperature data with hydraulic head measurements to provide more reliable estimates of vertical groundwater fluxes as opposed to one method alone (Schmidt et al. 2007; Essaid et al. 2008; Anibas et al. 2011; Hyun et al. 2011).

According to previous research (Jiang et al. 2015), the stream morphology is a significant factor controlling erosional and depositional conditions and spatial variability of streambed vertical hydraulic conductivity in the Beiluo River, in Shaanxi Province, China. The spatial variability of streambed vertical hydraulic conductivity can cause high spatial variability of vertical water fluxes (Conant 2004). Measurements of streambed vertical hydraulic conductivity and water fluxes have been carried out in the Beiluo River (Song et al. 2016), which focused on the heterogeneity of streambed hydraulic conductivity and vertical water fluxes only in an anabranching channel using one method of Darcian flux calculations. However, so far, there is no comprehensive small-scale survey relating spatial variability in vertical streambed water fluxes to

different streambed morphologies using multiple methods; hence, determination of the streambed hydraulic conductivity and vertical streambed water fluxes in different stream morphologies are crucial to estimate groundwater/surface-water interaction as well as being highly beneficial for stream ecosystems in the hyporheic zone. Consequently, this study extends the work of Song et al. 2016 by investigating spatial variability of vertical streambed water fluxes at three different streambed morphologies (near a meander bend, in an anabranching channel and in a straight stream channel). The main objectives of this study are to (1) quantify streambed vertical hydraulic conductivity and water fluxes at small scale, and their spatial variability, (2) relate their variability to different channel morphologies and (3) compare the performance of the two methods (Darcian flux calculations and vertical streambed temperature profiles) by making measurements near the same locations.

Field sites

The field study was conducted along a 13.5-km section in the Beiluo River (Fig. 1). Field measurements took place in January 2015. To relate spatial variability in vertical streambed water fluxes to differences in stream morphology, three test stream sections were selected for investigation: meander bend (MB) site, anabranching channel (AC) site, and straight channel (SC) site (Fig. 1). Each test stream section had characteristic stream morphology: MB site was located near a meander bend with relatively higher sinuosity compared with the other two test sites (Fig. 1; Table 1); AC site was located approximately 10 m downstream of an anabranching channel, and a 13 m long sand bar was presented in the center of the anabranching channel divided into two parts (Fig. 1d; Table 1); SC site was located in a straight stream channel that was straighter than the channel at the AC site (Fig. 1; Table 1). The Beiluo River is one of the largest tributaries of the Weihe River and is a meandering stream that flows from northwest to southeast into the Weihe River. The Beiluo River has a length of 680 km and catchment area of 26,900 km², and the basin has a continental monsoon climate. The annual mean precipitation and mean temperature are 541.7 mm and 13.2 °C, respectively. The average river gradient is 1.98‰ and the average stream flow is 14.99 m³/s. The Beiluo River Basin lies in the transition region between the Loess Plateau and the Guanzhong Basin. The streambed sediments comprise predominantly loess sandy clay, and sand-gravel of Pliocene/Holocene age. A variety of stream geomorphologies such as straight channel, anabranching channels, meander bends, point bar, and cut bank in the Beiluo River are developed because of the change from a predominantly erosional regime to a predominantly depositional regime. These different stream morphologies and contrasting erosional and depositional conditions would lead to different grain-size

distributions of streambed sediments, which have significant influence on streambed hydraulic conductivity and water fluxes in the hyporheic zone.

The Beiluo River flows from north to south with many sharp bends in the channel (Fig. 1b). Due to those bends, one stream bank is being eroded while sedimentation processes take place at the opposite bank. The erosional bank was located on the left side of the channel at the MB site, and the right sides of the channel at the AC site and the SC site, respectively (Fig. 1c–e). Each site was a 75–100 m long stretch of the river divided into four to five transects of about 30 m length perpendicular to the river. Each transect contained five measurements positioned approximately at similar locations (E1: near the erosional bank, E2: between the erosional bank and the center of the channel, C: center, D2: between the depositional bank and the center of the channel, D1: near the depositional bank). A total of 65 measurements at three test sites were conducted to determine spatial distribution of vertical streambed water fluxes in January 2015. Having four to five transects and five evenly spaced test locations across each transect can provide observations of a wider range of spatial variability of vertical streambed water fluxes at three different stream morphologies. Figure 1c–e shows the measurement locations of each test site. The identified measurement locations are also displayed in the contour maps of streambed topography (Fig. 1f–h), K_v , VHG and fluxes (Fig. 3). Table 1 details the hydrological condition and geomorphologies at each test site.

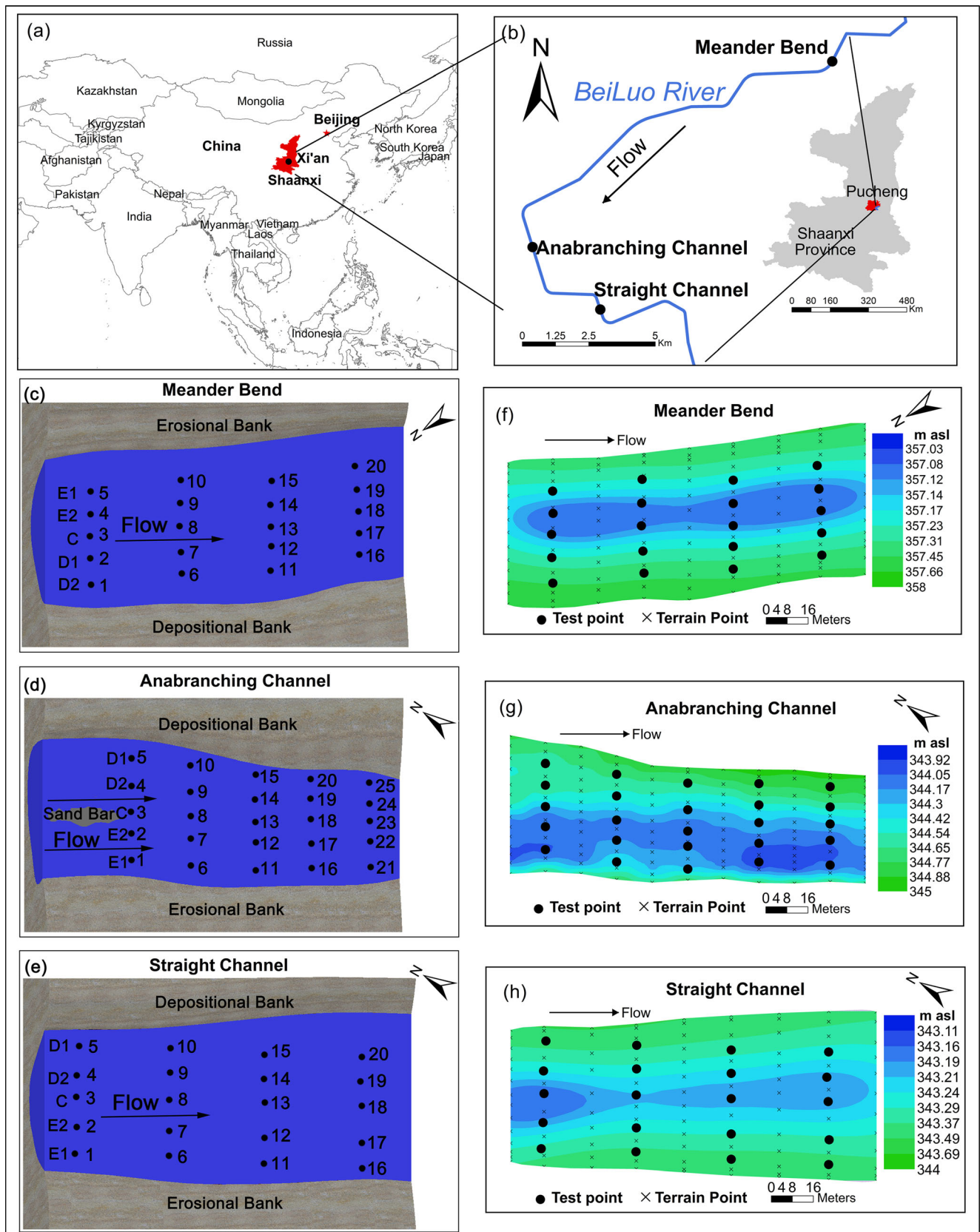
Methods

Streambed K_v , vertical hydraulic gradient, and estimation of vertical flux

In situ falling-head permeameter tests were applied to measure streambed K_v (Chen 2004; Chen et al. 2009). A transparent polyvinyl chloride (PVC) standpipe of 160 cm length and 5.4 cm diameter was inserted vertically to approximately 30 cm depth below the streambed, thus trapping a sediment column of 30 cm length. After allowing the water in the pipe to equilibrate, stream water was poured carefully from the open top of the pipe to create a hydraulic head. Then hydraulic heads at given time intervals were recorded along with falling of the water level in the pipe (Fig. 2c). Streambed K_v values were calculated from Hvorslev (1951):

$$K_v = \frac{\pi D}{11m} + L_v \ln\left(\frac{h_1}{h_2}\right) \quad (1)$$

where h_1 and h_2 are the hydraulic heads inside the pipe measured at times t_1 and t_2 , respectively, $m = \sqrt{K_h/K_v}$,



K_h is the horizontal conductivity of the streambed sediment, L_v is the length of the sediment column in the

pipe (30 cm), and D is the interior diameter of the pipe (5.4 cm). Thus, the ratio (L_v/D) is larger than 5 in this study.

◀ **Fig. 1 a–b** Map of the study sites within Shaanxi Province, China. The conceptual diagrams of the **c** meander bend, **d** anabranching channel and **e** straight channel, and measurement locations are shown. Streambed topography and its measurement locations are also shown at the **f** meander bend, **g** anabranching channel, and **h** straight channel. **c–e** The position across the stream is shown. *E1*: near the erosional bank, *E2*: between the erosional bank and the center of the channel, *C*: center, *D2*: between the depositional bank and the center of the channel, *D1*: near the depositional bank

A simplified version of Eq. (1) can be provided by Chen (2004) such that

$$K_v = \frac{L_v}{t_2 - t_1} \ln\left(\frac{h_1}{h_2}\right) \quad (2)$$

and the error of the modified calculation will be less than 5% for any anisotropic sediments (Chen 2004). For more detail, a full description of the equation can be found in Chen (2004).

Before the K_v test, hydraulic heads were measured in the pipes 16 h after the installation. VHG was derived by dividing differences in hydraulic heads by the thickness of the sediment core (Chen et al. 2009):

$$i = \frac{\Delta h}{L_v} \quad (3)$$

where Δh is the hydraulic head difference between stream water level and water level in the pipe, L_v is thickness of the sediment core in the pipe, and i is the value of vertical hydraulic gradient.

Upward hydraulic gradient demonstrates gaining conditions, indicating streambed supplying water to the river (Fig. 2a), whereas downward hydraulic gradient demonstrates losing conditions, indicating infiltration of stream water into the streambed (Fig. 2b), and no hydraulic gradient indicates that there can be no flow of water across the streambed.

Then, the vertical streambed water fluxes q_v at each test location can be calculated using the value of vertical hydraulic gradient i and vertical hydraulic conductivity K_v according to Darcy's law (Chen et al. 2009):

$$q_v = i \times K_v \quad (4)$$

Vertical sediment temperature profiles and estimation of vertical flux

In the wintertime, the temperature distribution in the sediments approaches the most optimal thermal steady state due to the smallest diurnal oscillations and relatively constant long-term trends of surface water temperatures (Conant 2004; Schmidt et al. 2007; Anibas et al. 2009). Hence, a winter temperature measurement campaign was conducted along the Beiluo River on 8, 17, 19 January 2015 with a 0.8-m-long self-made temperature probe along with in situ Darcy measurements at locations very close by. Vertical sediment temperature profiles were measured with a vertical probe

Table 1 Hydrological condition and geomorphologies of test sites

Parameter	Site		
	MB	AC	SC
Test date	January 17, 2015	January 8, 2015	January 19, 2015
Number of measurements	20	25	20
Average channel width (m)	32.7	33.4	31.7
Site length (m)	79	100	76.5
Max. water depth (cm)	105	117	96
Average water depth (cm)	62.2	48.2	59.6
Stream gradient (m/m)	2.4‰	1.8‰	1.8‰
Sinuosity	1.08	1.01	1.01
Average thickness of measured sediment (cm)	30.7	30.3	30.7
Mean water depth of E1/E2/C/D2/D1 (cm)	86/80.5/81/76.5/71.3	80.9/77.5/71.3/39.8/19.2	76/74.3/74/72/72
Site description	Test site is near a meander bend. Streambed sediment contains medium sand, and a small part of silt and clay particles, with the exception of D1 location, where streambed sediment contains medium sand, and large part of silt and clay	Test site is located in 10 m downstream of an anabranching channel. Stream flow is divided into two branches by a 13-m sand bar. Streambed sediment contains large part of sand and a small part of gravel, with the exception of E2 location, where streambed sediment contains medium sand, large part of silt and clay, and a small part of gravel	Streambed sediment contains medium sand, silt and clay particles, with the exception of C location, where streambed sediment contains medium sand, small part of silt and clay, and gravel

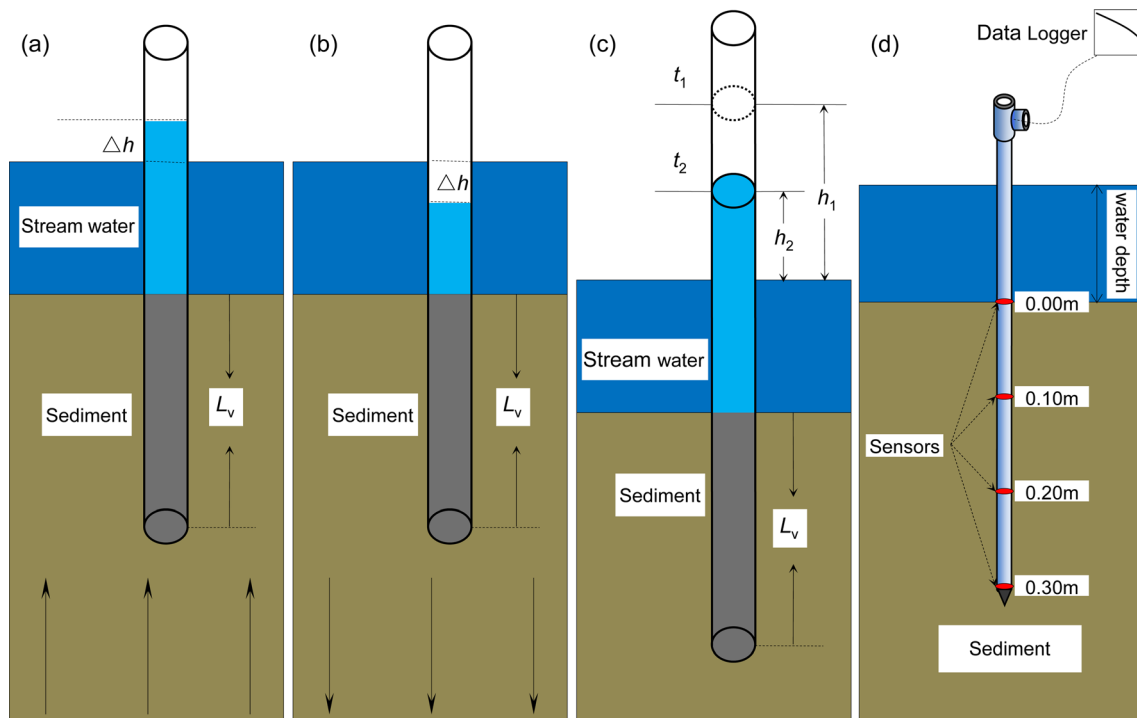


Fig. 2 Schematic diagrams showing: **a** vertical head gradient measurement (upward flow); **b** downward flow; **c** an in situ permeameter test to determine streambed K_v ; and **d** vertical temperature measurement in the streambed with a temperature probe

consisting of four temperature sensors (accuracy 0.05 °C) located at the water–sediment interface (0 m), 0.1, 0.2, 0.3 m depths in the streambed at each location (Fig. 2d). A total of 65 temperatures profiles were collected at the three test sites.

Under steady-state conditions with vertical flow, the analytical solution of the one-dimensional (1D) steady convective-conductive heat transport equation derived by Bredehoeft and Papaopulos (1965) was used for estimating the vertical streambed fluxes on the basis of vertical temperature profiles in the streambed:

$$\frac{T_z - T_0}{T_L - T_0} = \frac{\exp\left(\beta \frac{z}{L}\right) - 1}{\exp(\beta) - 1} \quad (5)$$

where T_z is the streambed temperature at a given depth z ; T_0 and T_L represent the measured temperatures at the upper and lower boundaries, respectively; L is the vertical length of the measured sediment bed; β is the Peclet number. To avoid the influence of diurnal stream-water-temperature oscillations at the 0.0 m depth, T_0 at the upper boundary is defined as the temperature value of the respective temperature profile 0.1 m depth below the streambed surface (Schmidt et al. 2006; Anibas et al. 2011). The groundwater temperature at a depth of 4 m below the streambed surface approaches constant values (Anderson 2005). Hence, the lower boundary was set to 5 m below the streambed surface for assuming a thermal steady state of

the groundwater temperature T_L ($L = 5$ m). At each test site, groundwater temperature was measured in a nearby well.

The Peclet number β indicates the ratio of convection to conduction:

$$\beta = \frac{c_w \rho_w v_z L}{K_{sw}} \quad (6)$$

where $c_w \rho_w$ is the volumetric heat capacity of water [$\text{J}/(\text{m}^3 \text{K})$], K_{sw} is thermal conductivity of the solid-water matrix [$\text{J}/(\text{sm K})$], v_z is the vertical component of Darcian flux in the sediment (m/s). For convenience, the units mm/d are used to express fluxes. β is positive or negative depending on whether the vertical streambed water flux v_z is positive (downward flow) or negative (upward flow). For $\beta = 0$, groundwater flow does not occur, and the heat transport process is dominated by conduction almost exclusively and not advection/convection.

The optimum value of β is determined by assigning an initial value to β and then adjusting it until the sum of squared difference between the left and right sides of the Eq. (5)—i.e. the objective function $F(\beta)$ is minimized (Saleem 1970)—where

$$F(\beta) = \sum_{z=0}^{z=L} \left[\frac{T_z - T_0}{T_L - T_0} - \frac{\exp\left(\beta \frac{z}{L}\right) - 1}{\exp(\beta) - 1} \right]^2 \quad (7)$$

The Solver add-in in Microsoft Excel was used to solve Eq. (7) with the approach of Arriaga and Leap (2004).

Once the optimum value of β was derived from the method as described in the preceding, vertical streambed water flux v_z (mm/d) can then be estimated by the following equation:

$$v_z = \frac{K_{sw}\beta}{c_w\rho_w L} \quad (8)$$

where the parameters used are given in Table 2. The thermal conductivity K_{sw} and specific heat capacity of water c_w were obtained by making direct measurements on sediment and water samples at each site (Table 2). Streambed water fluxes with $|\beta| < 0.5$ were estimated as zero due to measurement difficulty of too small fluxes using temperature profiles (Bredhoeft and Papaopulos 1965). The steady-state approximation is only reliable and quantitative for gaining conditions (Anibas et al. 2011; Schmidt et al. 2007). Although downward fluxes can be calculated according to Eq. (8), such estimates should be seen more qualitatively. Hence, the results for downward fluxes obtained from vertical temperature profiles can only be used to indicate possible losing conditions in the interpolated maps (Fig. 3d,h,l), but cannot be used for any statistical analysis in this study.

Streambed topography

At each test site, a Topcon GTS-102 N construction total station was used to detect the streambed topography (streambed elevation in meters above sea level). The detection of angle is obtained by 2 horizontal and 1 vertical measurements, and the prism mode-of-measurement accuracy is $\pm (2 \text{ mm} + 2 \text{ ppm} \times D)$ mean squared error (MSE).

Sediment cores analysis

A total of 15 sediment cores were collected for grain size analysis. These cores were sampled from 15 in situ permeameter test locations in the streambed among the 65 test locations. At the MB site, five cores were sampled from test locations 1, 2, 3, 4, and 5 (Fig. 1c). At the AC site, five cores

were sampled from test locations 1, 2, 3, 4, and 5 (Fig. 1d). At the SC site, five cores were from test locations 16, 17, 18, 19, and 20 (Fig. 1e). Sediment samples in the laboratory were air-dried and sieved using 17 grades. The finest grain size was 0.075 mm and the coarsest grain size was 12 mm. The grain was classified into three groups: silt or clay (size < 0.075 mm), sand ($0.075 \text{ mm} \leq \text{size} \leq 2 \text{ mm}$), and gravel (size > 2 mm).

Contour maps and statistical analysis

The contour maps of streambed topography, K_v , VHG and fluxes based on the two methods were generated using the ordinary Kriging interpolation technique and Gaussian Kernel Function (Merwade et al. 2006) with ArcGIS 10.1 software (Figs. 1 and 3). The errors of interpolation are generally lower than 10% except at the AC site where the errors of streambed K_v and fluxes based on the two methods are greater than 10%. In general, the errors of interpolation are considered relatively acceptable in this study.

All statistical analyses were performed using the statistical software program R 3.2.1 (R Core Team 2016). The Kruskal-Wallis test (Helsel and Hirsch 1992) is a nonparametric test that is valid even for non-normal populations. In this report, the Kruskal-Wallis test was used to determine if there is significant difference at a 95% confidence level for upward water fluxes based on Darcian flux calculations and vertical temperature profiles at the same test site. The Kruskal-Wallis test was also used to determine if there is significant difference at a 95% confidence level between upward water fluxes based on Darcian flux calculations, or upward water fluxes based on vertical temperature profiles or corresponding streambed K_v values or VHG values at two test sites. The test null hypothesis is that streambed K_v values, or VHG values, or water fluxes from two samples are drawn from the same population, and the alternative hypothesis is that data from two samples are significantly different.

The complex dynamic pattern of upward flux and downward flux in the hyporheic zone can be caused by

Table 2 Parameter values used for determining vertical streambed water fluxes v_z at each site

Parameter	Value			
	Site MB	Site AC	Site SC	Units
Thermal conductivity, K_{sw} ^a	1.588	1.723	1.618	J/(sm K)
Specific heat capacity of water, c_w ^a	4,224	4,224	4,224	J/(kg K)
Density of water, ρ_w	1,000	1,000	1,000	kg/m ³
Upper boundary condition, T_0 ^b	Variable	Variable	Variable	°C
Lower boundary condition, T_L ^c	13.7	14.7	13.4	°C

^a Obtained by making direct measurements at each site

^b Located at 0.1 m below the interface between surface water and streambed

^c Measured in a nearby well, and assumed to be located at 5.0 m depth below the interface between the surface water and streambed for the steady-state analysis (Anibas et al. 2011)

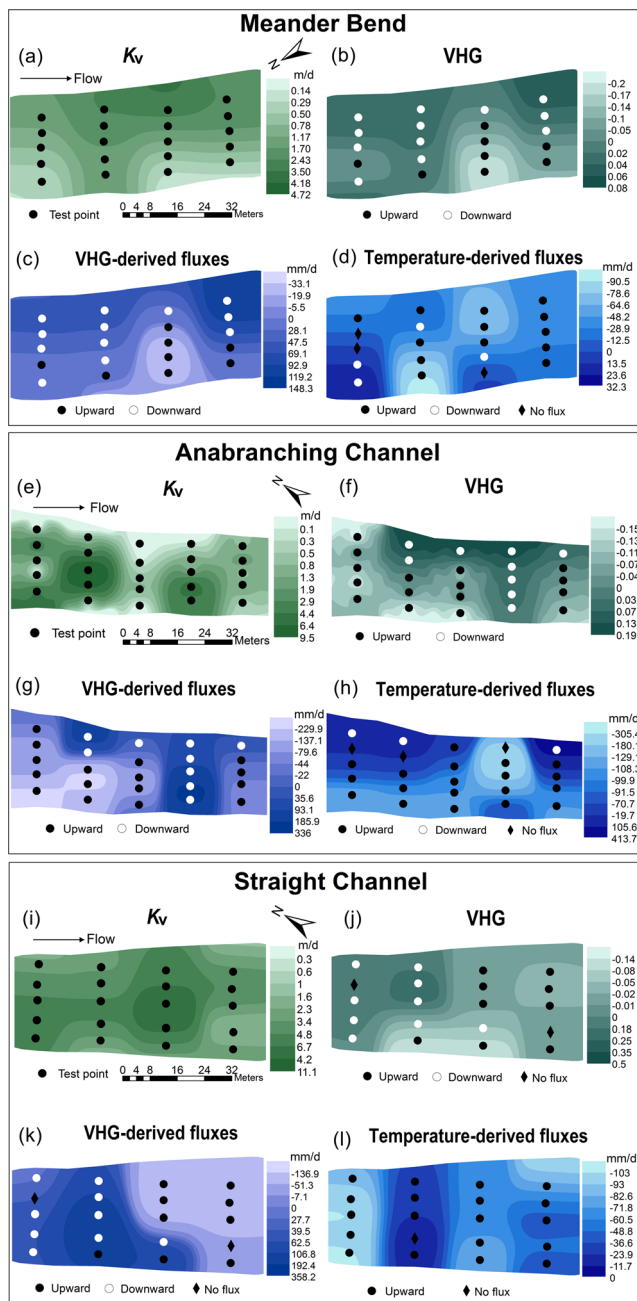


Fig. 3 Interpolated contour maps of K_v , VHG, VHG-derived fluxes and temperature-derived fluxes for each test site along the Beiluo River: **a–d** Meander bend (MB), **e–h** Anabranching channel (AC), **(i–l)** Straight channel (SC)

heterogeneous streambed hydraulic conductivity and hydraulic gradient (Chen et al. 2009). Hence, a non-parametric Spearman's rank correlation test (Helsel and Hirsch 1992) was used to examine if estimated fluxes based on the two approaches are significantly correlated to streambed K_v values or VHG values. The Spearman's rank correlation test was also used to examine if streambed K_v values are significantly correlated to VHG values. Moreover, streambed K_v is mainly controlled by grain size (Song et al. 2007), thus different grain

size distribution can affect streambed K_v , then affecting streambed water fluxes. Hence, the Spearman's rank correlation test was also used to examine if silt-clay content of the sediment are significantly correlated to the corresponding streambed K_v and vertical water fluxes.

Results

Spatial variability of vertical hydraulic conductivity and vertical hydraulic gradient

The streambed K_v values vary with different intensity at three individual sites (Table 3). Generally, at the MB site, the K_v values are higher near the erosional bank than those in the center of the channel and near the depositional bank (Fig. 3a). At the AC site, higher streambed K_v values occur close to the erosional bank and in the center of channel (Fig. 3e). At the SC site, higher K_v values are observed closer to the center of the channel (Fig. 3i).

VHG values show different variability of upward gradients and downward gradients at each test site (Table 3). There is also a clear distinction of VHG values between the erosional and depositional bank of the stream at three sites. At the MB site, larger upward gradients are observed close to the depositional bank in the downstream part and larger downward gradients are observed close to the erosional bank (Fig. 3b). At the AC site, VHG values show larger upward gradients near the erosional bank and lower upward gradients close to the center of the channel (Fig. 3f). Larger downward gradients are observed near the depositional bank and lower downward gradients are observed in the sink area in the streambed topography (Fig. 3f). Whereas at the SC site, VHG values show relatively larger upward gradients near the erosional bank and lower upward gradients at the downstream part (Fig. 3j). Downward gradients are observed at the upstream part of the reach (Fig. 3j).

Spatial variability of VHG-derived fluxes

The VHG-derived fluxes, calculated using Darcian flux calculations, exhibit spatial variability at three sites (Table 4). Only at two locations of the SC site, water flow across the streambed is not observed (Fig. 3k). Results indicate that significant spatial variations in direction and magnitude of streambed fluxes are observed along the channel and across the channel over the reach of interest on a 0.3 m small scale at three sites (Fig. 3c,g,k). At the MB site, the fluxes distribution shows higher upward fluxes near the depositional bank in the downstream part and higher downward fluxes near the erosional bank (Fig. 3c). At the AC site, a flux pattern is observed with upward fluxes in the step and downward fluxes in the sink in the streambed topography (Fig. 3g). Higher upward

Table 3 Statistics for K_v and VHG values at the three test sites

Site	K_v				VHG			
	Min (m/d)	Max (m/d)	Mean (m/d)	Median (m/d)	Min	Max	Mean	Median
MB	0.04	4.72	1.39	1.14	-0.22	0.08	-0.03	0.02
AC	0.03	9.52	2.17	1.11	-0.18	0.19	-0.02	-0.04
SC	0.04	11.1	4.49	4.70	-0.21	0.05	-0.02	0

fluxes are observed near the erosional bank in the upstream part, whereas higher downward fluxes are observed near the sink center and near the depositional bank (Fig. 3g). However, at the SC site, higher upward fluxes are observed from the channel center towards the depositional bank in the downstream part, and higher downward fluxes are observed from the channel center towards the erosional bank in the upstream part (Fig. 3k). Note that changes from upward to downward flow occur in the neighboring two locations about 5 m apart across the stream or about 20 m apart along the stream at each site (Fig. 3c,g,k).

Streambed temperature and groundwater temperature

At the water–sediment interface (0.0 m), the temperatures vary between 2.1 and 4.6 °C at the MB site, between 3.7 and 8.4 °C at the AC site, between 3.7 and 5.2 °C at the SC site. At the maximum depth (0.3 m), the streambed temperatures are observed to be between 5.0 and 5.8 °C at the MB site, between 4.9 and 7.7 °C at the AC site, and between 5.6 and 6.5 °C at the SC site. The temperature differences between the interface and the maximum depth vary between 1.0 °C and 3.1 °C (average = 1.9 °C, median = 2.1 °C) at the MB site, between 0.8 and 3.4 °C (average = 2.3 °C, median = 2.6 °C) at the AC site, and between 0.8 and 2.6 °C (average = 1.7 °C, median = 1.7 °C) at the SC site. Hence, the temperature differences between the interface and the maximum depth are obtained at three sites. Figure 4 shows the measured temperature profiles for strongly gaining and losing conditions at the three test sites. Groundwater temperatures are respectively 13.7 °C at the MB site, 14.7 °C at the AC site, and 13.4 °C at the SC site (Table 2).

Spatial variability of temperature-derived fluxes

The temperature-derived fluxes, calculated using vertical temperature profiles, also exhibit spatial variability at three sites (Table 4). Water flow across the streambed was not observed at three locations of the MB site (Fig. 3d), three locations of the AC site (Fig. 3h), and one location of the SC site (Fig. 3l). Results indicate that water fluxes at three sites usually show gaining conditions, suggesting that the stream mainly gains water from adjacent aquifers over the reach of interest (Fig. 3d,h,l). At the MB site, downward fluxes partly appear near the depositional bank, while lower upward fluxes generally appear from the center of the channel towards the erosional bank, and higher upward fluxes are observed near the depositional bank at the upstream part (Fig. 3d). At the AC site, downward fluxes appear near the depositional bank, while lower upward fluxes generally appear from the center of the channel towards the erosional bank, and higher upward fluxes are observed near the depositional bank at the downstream part (Fig. 3h). At the SC site, no downward fluxes are observed, while higher and lower upward fluxes appear alternately along the flow direction (Fig. 3l).

Correlations between fluxes and K_v values and VHG values

There are no significant correlations between K_v and VHG-derived fluxes at the AC site and at the SC site. A positive correlation between K_v and VHG-derived fluxes is revealed at the MB site ($R = 0.56, p = 0.01$), suggesting that K_v may represent a reliable measure of streambed water fluxes, at least at

Table 4 Statistics for VHG-derived fluxes and temperature-derived fluxes at the three test sites

Site	Upward fluxes (VHG)				Downward fluxes (VHG)				Upward fluxes (temperature)				Downward fluxes (temperature)			
	Min (mm/d)	Max (mm/d)	Mean (mm/d)	Median (mm/d)	Min (mm/d)	Max (mm/d)	Mean (mm/d)	Median (mm/d)	Min (mm/d)	Max (mm/d)	Mean (mm/d)	Median (mm/d)	Min (mm/d)	Max (mm/d)	Mean (mm/d)	Median (mm/d)
MB	-4.1	-47.5	-21.2	-18.3	10	148.3	64.1	66.9	-20.5	-100.7	-57.7	-50.5	17.9	32.3	23.9	23.3
AC	-5.1	-380.0	-121.1	-89.9	6.4	336.0	106.4	67.3	-32.5	-613.5	-129.9	-114.6	57.0	413.7	176.7	59.3
SC	-4.9	-302.7	-95.4	-56.1	25.7	358.2	138.6	75.0	-21.2	-112.6	-65.3	-66.9	-	-	-	-

– Downward fluxes were not observed at the site SC using vertical temperature profiles

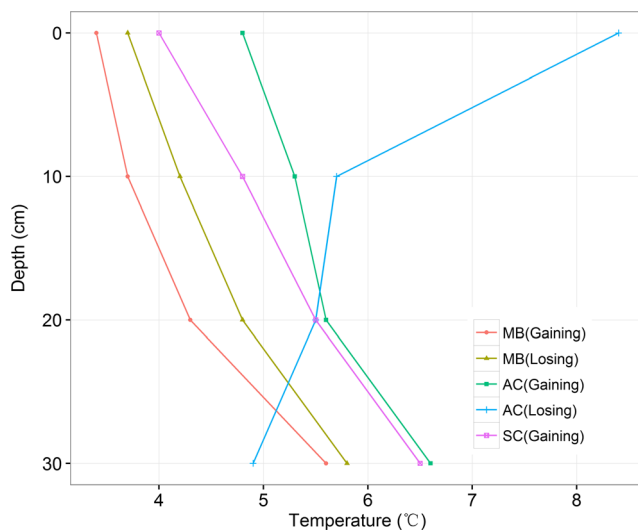


Fig. 4 The measured temperature profiles for strongly gaining and losing conditions at each test site

some test sites. The correlation coefficients of VH_G and VH_G-derived fluxes at the 0.05 level are 0.83 at site MB ($p < 0.001$), 0.54 at site AC ($p = 0.006$), and 0.87 at site SC ($p < 0.001$), indicating significant positive correlation between VH_G and VH_G-derived fluxes at each site. This could imply that VH_G can be a better indicator of the intensity of VH_G-derived fluxes than K_v at the three test sites; however, the results make little difference to the significance or trend of the relationships between VH_G-derived fluxes and K_v or VH_G when only considering upward fluxes derived from the two approaches. A significant positive correlation exists between K_v and VH_G-derived upward fluxes at the AC site ($R = 0.90$, $p < 0.001$) and at the SC site ($R = 0.93$, $p < 0.001$) and no significant correlations between VH_G and VH_G-derived upward fluxes are found at any of the sites. In contrast to these results, no significant correlations are detected between temperature-derived upward fluxes and streambed K_v or VH_G values at any of the sites. Moreover, a significant inverse correlation exists between K_v and VH_G values at the MB site ($R = -0.78$, $p < 0.001$) and at the AC site ($R = -0.80$, $p < 0.001$); the smaller the K_v , the higher the VH_G.

Correlations between grain size and K_v values or fluxes

Due to the small amount of sediment-core data (15 samples) and the requirement of gaining conditions based on the temperature profiles, only the correlation between silt-clay content of the sediment and VH_G-derived fluxes was examined. As expected, the Spearman's rank correlation test shows that silt-clay content of the sediment correlates significantly negatively with streambed K_v ($R = -0.50$, $p < 0.05$) and vertical fluxes ($R = -0.57$, $p < 0.05$).

Discussion

Comparison of the two approaches for estimating water fluxes

At 37 of the 65 test locations, the directions of calculated water fluxes using Darcian flux calculations are not consistent with those obtained by vertical temperature profiles. This may be largely related to the variations of head gradient and streambed temperature over time. Head gradients within a 16-h period were temporally variable in response to stream fluctuation and thus uncertainty in the head gradients contributed to increase the uncertainty over the direction of Darcian fluxes. Also, the temperature at the time of temperature measurements may be different from the temperature during the time of Darcy measurements. Shallow streambed temperatures are mainly influenced by surface diurnal temperature variations, and shallow streambed temperatures change more quickly with time than with depth (Hyun et al. 2011), thus the discrepancy in temperature measurements may also lead to uncertainty in the temperature-derived fluxes. Furthermore, at a few test locations—for example, test locations MB2 and MB12 in Fig. 3d, and AC5 in Fig. 3h—some temperature cycling through shallow streambed sediments may be produced by heat conduction despite upward Darcian fluxes observed in Fig. 3c,g (Storey et al. 2003); however, a temperature variation of 10–15% at 20 cm depth could only be attributed to heat conduction, even with no vertical water flow (Silliman et al. 1995). Also, the upward gradients (test locations SC4 and SC17, Fig. 3l) may be too small to be detected by measurements in the pipes (Fig. 3k). Moreover, the low-permeability streambeds at some test locations (For example, MB3 in Fig. 3a and AC15 in Fig. 3e) may also prevent water flow infiltration into sediments, causing that downward fluxes had little influence on heat transport (Fig. 3c,d,g,h), although downward fluxes were observed by VH_Gs measurements (Hyun et al. 2011). Rau et al. (2010) also showed that heterogeneity in streambed hydraulic conductivity is a possible cause for the discrepancy of flux direction estimated by temperature time series and Darcian flux calculations.

At 28 of the 65 test locations, values of VH_G-derived fluxes and temperature-derived fluxes are negative, indicating gaining conditions. At the 28 test locations, values of VH_G-derived upward fluxes range from -380.0 to -4.1 mm/d, and show greater variability than the range from -132.6 to -20.5 mm/d of temperature-derived upward fluxes. The differences between estimated upward fluxes based on the two approaches have many possible causes. In order to avoid sediment disturbance, the temperature and Darcy measurements were carefully carried out at slightly different locations; thus, this may have affected differences of the fluxes based on the two methods, but it seems unlikely that it would be responsible for large differences. Relatively large differences may be

associated with the different nature of the two approaches. The approach of Darcian flux calculations strongly depends upon the heterogeneity in streambed hydraulic conductivity, often varying over a few orders of magnitude, while the approach of vertical temperature profiles needs knowledge on the thermal conductivity that has much lower variability than hydraulic conductivity (Duque et al. 2015). As Dujardin et al. (2014) also stated, discrepancies of water fluxes between the hydraulic gradient method and the thermal method are caused by the uncertainty of streambed hydraulic conductivity. The approach of using vertical temperature profiles tends to underestimate or overestimate VHG-derived upward fluxes at some test locations (Fig. 5), possibly due to violation of the assumptions of steady-state conditions (Schmidt et al. 2007; Anibas

et al. 2009; Schornberg et al. 2010). At the areas with high groundwater discharge, streambed temperature and groundwater temperature are very close, and the application of the 1D heat transport equation would derive the minimum flux but the true flux could be doubled or tripled; whereas at the areas with low groundwater discharge, too shallow temperature measurement depths (30 cm for this study) may also provide erroneous flux estimates (Schmidt et al. 2007). For example, the low VHG-derived upward fluxes occur near the depositional bank at the SC site with low K_v values and lowest VHG values observed (Fig. 5i,j,k), however, where the temperature-derived upward fluxes are highest (Fig. 5l). Irvine et al. (2015) and Birkel et al. (2016) also reported that the application of the 1D heat equation may be problematic

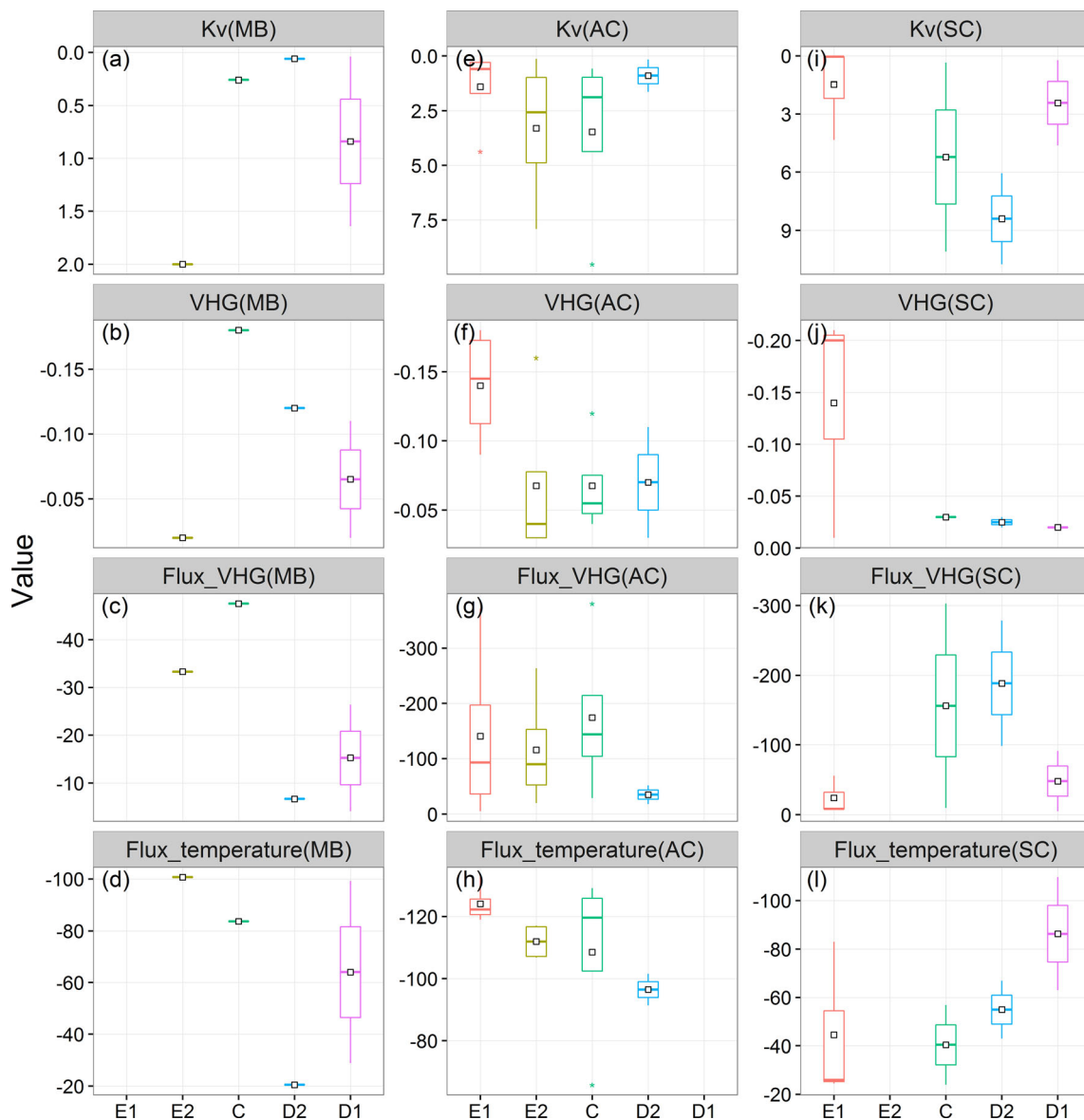


Fig. 5 Box plots of K_v , VHG, VHG-derived fluxes and temperature-derived fluxes from each upward position across the stream at each test site: **a–d** Meander bend (MB), **e–h** Anabranching channel (AC), **i–l**

Straight channel (SC). All K_v magnitudes are in m/d. All water flux magnitudes are in mm/d

due to violation of the assumptions of homogeneity and purely vertical flow. Other possible factors like variations in streambed topography (Swanson and Bayani Cardenas 2010) and the complex hyporheic flow paths may also lead to violation of the one-dimensional assumption.

Nonetheless, in order to reduce measurement errors of the Darcy method proposed in this study, it can take more than 1–2 h or an even much longer time for the water in the pipe to reach equilibrium. For each test site, a large number of pipes were inserted into the streambed at all test locations in a relatively short time; thus, the hydraulic head differences were recorded from a large quantity of tests at a given time. For reducing the influence of surface-water temperature and streambed heterogeneity, deeper temperature and Darcy measurements are also very necessary to obtain more exactly water fluxes based on the two methods if the stream water during the field test is not very muddy and deep.

Despite the different water-flux estimates, the Kruskal-Wallis tests show no significant differences of upward fluxes based on the two approaches at each test site. This verifies the approach of using vertical temperature profiles with Darcian flux calculations. The lowest absolute difference between the resulting upward fluxes obtained from vertical temperature profiles and Darcian flux calculations is 13.8 mm/d at the MB site, 9.2 mm/d at the AC site, and 14.1 mm/d at the SC site, respectively. Anibas et al. 2011 also reported similar lowest absolute difference between the estimated fluxes based on hydraulic head gradients and temperature data. The average and median differences between the resulting upward fluxes based on the two approaches are less than 60 mm/d at the three test sites, and of little practical importance, which also shows that both approaches are applicable for estimating vertical water fluxes.

Spatial variability of the upward fluxes based on vertical temperature profiles and the Darcian flux calculations show many similarities. The upward fluxes based on the two approaches and K_v or VHG also show relatively similar spatial variability. At the MB site, the upward fluxes are higher from the center of the channel towards the erosional bank (Fig. 5c,d), where higher K_v values or higher VHG values are observed (Fig. 5a,b). The relatively lower upward fluxes are observed between the depositional bank and the center of the channel (Fig. 5c,d), where lower K_v values are observed (Fig. 5a). At the AC site, higher upward fluxes are observed near the erosional bank and in the center of channel (Fig. 5g,h), where higher VHG values or higher K_v values are observed (Fig. 5e,f). The relatively lower upward fluxes are also observed between the depositional bank and the center of the channel (Fig. 5g,h), where lower K_v values are also observed (Fig. 5e). At the SC site, higher upward fluxes are observed from the center of the channel towards the depositional bank where higher K_v values are observed (Fig. 5k,l). The relatively lower upward fluxes are observed near the

erosional bank (Fig. 5k,l), where lower K_v values are observed (Fig. 5i). At each test site, much more range of upward fluxes is observed at locations where much more range of K_v values or VHG values is also observed (Fig. 5). Hence, high fluxes are mostly observed from the center of the channel towards the bank or even near the bank, again indicating that the bank zones are of significant importance in groundwater/surface-water interaction (Anibas et al. 2011). High fluxes can be also observed in the center of the channel. Correspondingly, Flewelling et al. (2012) also measured high specific discharge of groundwater in the thalweg of a stream using seepage meters.

Moreover, at the AC site, the spatial distribution of flux directions obtained by these two methods is relatively similar, both showing upward fluxes in the step areas and downward fluxes near the depositional bank (Fig. 3g,h). At the SC site, flux directions based on the two methods also show upward fluxes in the step areas in the downstream part (Fig. 3k,l). Similarly, Harvey and Bencala (1993) also found that upward paths were encountered where stream-water slope decreased. It is also apparent that upward and downward water fluxes can occur within a short distance, even at scales of only a few meters apart, especially for water flux estimates based on the Darcian flux calculations (Fig. 3c,g,k), which could imply that the groundwater and surface water actively mix and exchange in the hyporheic zone at the investigation time. At the three test reaches, regional groundwater discharge or recharge rates were probably not sufficiently high to prevent the inflow or outflow of surface water into the streambed on the local small-scale, as shown by Chen et al. 2009 and Hyun et al. 2011. Many researchers have also illustrated that upward and downward fluxes occurring at meter to tens of meter scales can be induced by bed topography and stream sinuosity (Vaux 1968; Savant et al. 1987; Cardenas et al. 2004), and spatial heterogeneities in streambed K_v and VHGs (Chen et al. 2009) and variations in stream discharge (Bartsch et al. 2014). Associated complex bed topography and channel patterns at each site (Fig. 1f,g,h) may result in different hydraulic gradients within the hyporheic zone and substantially change hyporheic exchange. In view of the previous discussion, the mechanisms affecting flux dynamic pattern in the hyporheic zone are truly complex, and can act together, therefore a better understanding of these mechanisms still requires further research.

Correlations between fluxes, K_v values and VHG values

Although the correlations between the upward fluxes and K_v or VHG are not always statistically significant at the $p = 0.05$ level, high upward fluxes are mostly observed at certain locations with high streambed K_v or VHG, whereas low upward fluxes are observed at certain locations with low streambed K_v . The Kruskal-Wallis tests show that there are no significant

differences between the VHG-derived upward fluxes or corresponding K_v values or VHG values at the three test sites. The results of the Kruskal-Wallis tests of the VHG-derived upward fluxes at each test site correspond to the results of the Kruskal-Wallis tests of K_v values or VHG values; hence, streambed K_v can be a good indicator of water fluxes at the field test sites, which agrees with the results of Anibas et al. 2011 and Hyun et al. 2011. Anibas et al. 2011 attributed changes in fluxes across the channel to changes in local-scale shallow groundwater flow and streambed K_v , whereas Binley et al. (2013) also reported a similar finding of significant control of hydraulic conductivity over the magnitude and spatial distribution of vertical fluxes. Hydraulic gradient can also be an indicator of water fluxes at some field test sites; however, it cannot serve as a simple indicator for heterogeneous streambeds in the Beiluo River, as suggested by Kennedy et al. 2009. Additionally, Käser et al. (2009) even suggested VHG can be a misleading indicator of the intensity of flow.

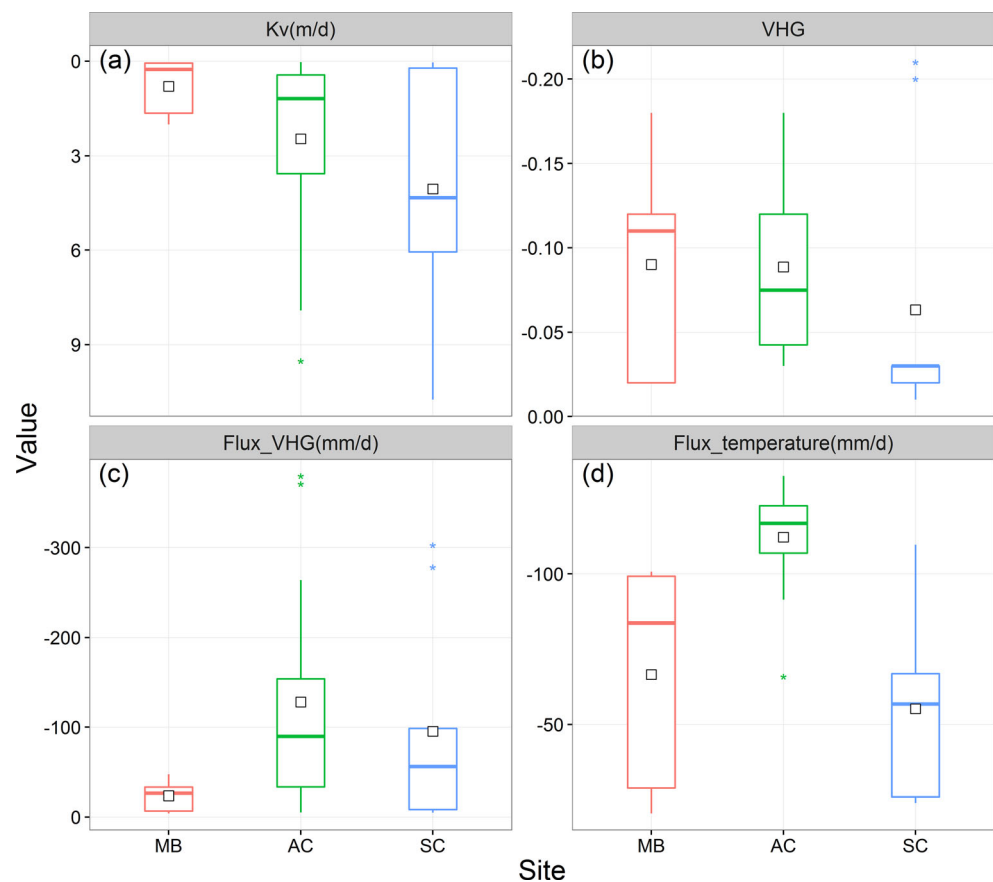
Streambed K_v values and VHG values are inversely related at the MB site and at the AC site. Similarly, Käser et al. (2009) and Sebok et al. (2015) also found an inverse correlation between K_v values and VHG values. The observed VHG values are the highest near the depositional bank in the downstream part of the MB site (Fig. 3a) and near the depositional bank at the AC site (Fig. 3e). In these areas, the streambed K_v values

are the lowest (Fig. 3b,f), possibly because low-permeability fine-grained sediments hindered the water exchange between groundwater and surface water. Generally, the highest upward fluxes can be expected at locations with high streambed K_v values and VHG values; however, among the three test sites, the highest upward fluxes are observed at the AC site which shows median streambed K_v values and VHG values (Fig. 6). VHG values are the highest at the MB site (Fig. 6b), which is also where upward fluxes are not the highest (Fig. 6c,d), most likely because of the lowest streambed K_v (Fig. 6a). Streambed K_v values are the highest at the SC site (Fig. 6a), but where upward fluxes are not also the highest (Fig. 6c,d), most likely because of the lowest VHG values (Fig. 6b).

Factors influencing K_v values and fluxes

The results of streambed K_v are in accordance with previous study of streambed K_v values at the three sites in June 2014 (Jiang et al. 2015), indicating higher streambed K_v values in the center of the channel and near the erosional bank (Fig. 3a,e,i). This is also consistent with the finding of Genereux et al. (2008) and Sebok et al. (2015). Genereux et al. (2008) additionally reported that the highest K_v values generally occurred in the center of the channel, while Sebok et al. (2015) also found higher K_v values on the erosional outer

Fig. 6 Box plots of **a** K_v , **b** VHG, **c** VHG-derived fluxes and **d** temperature-derived fluxes from all upward locations at the meander bend (MB), anabranching channel (AC), and straight channel (SC)



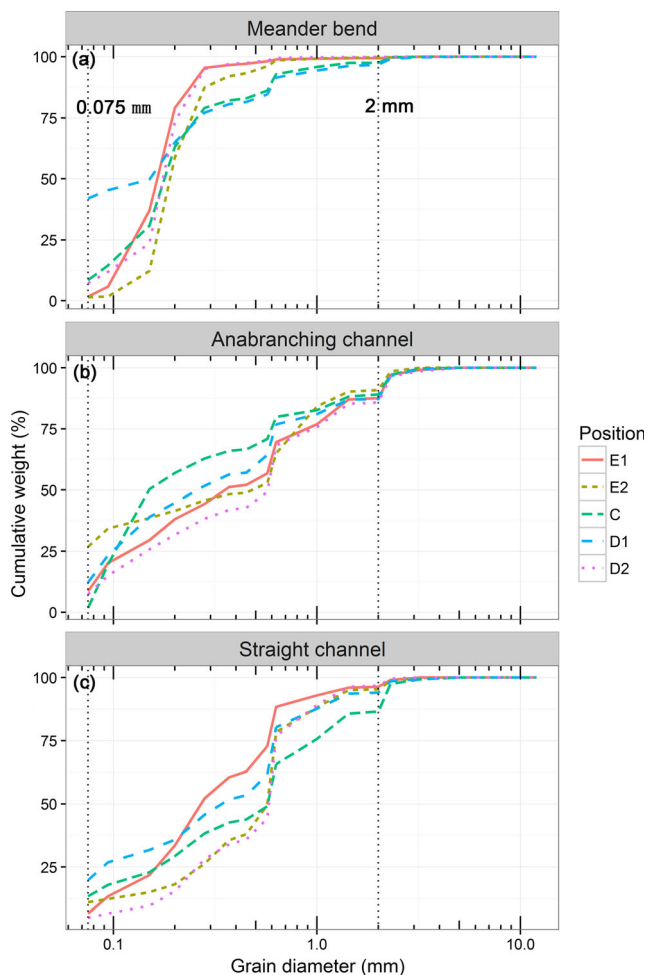


Fig. 7 The grain size distributions of five streambed sediment cores for each test site: **a** Meander bend, **b** Anabranching channel, **c** Straight channel

bend and near the middle of the channel compared to the depositional bank. Genereux et al. (2008) attributed differences in K_v across the channel to differences in streambed sediment grain size across the channel. In this study, the grain-size distribution varies significantly at different locations, even at the same test site (Fig. 7; Table 5), and this could result in different distribution of streambed K_v , and further affect the distribution of water fluxes. This is also confirmed

by the Spearman's rank correlation test, which shows the significant negative correlation between silt-clay content of the sediment and streambed K_v and VHG-derived fluxes. The link is in agreement with the results of Roque and Didier (2006), who found a negative exponential relationship between hydraulic conductivity and the weight of clay and silt; therefore, sediment grain size can be one of major controlling factors of streambed K_v and water fluxes at the three test sites.

Other complicating factors like sedimentary structures (Packman et al. 2006; Leek et al. 2009), clogging processes (Brunke and Gonser 1997; Blaschke et al. 2003), and hyporheic processes (Song et al. 2007; Rosenberry and Pitlick 2009; Chen et al. 2013) may also be related to the spatial distribution of streambed K_v and water fluxes. The structural characteristics of the streambed sediments can strongly influence hyporheic exchange (Leek et al. 2009), which was much more rapid with the high-permeability gravel than with the gravel–sand mixture (Packman et al. 2006). The formation of a clogging layer can lead to a reduction of pore volume and a decrease of streambed hydraulic conductivity, and thus reduces the hydrological connections between surface water and groundwater (Brunke and Gonser 1997). Upwelling flow in streambeds can possibly expand pore space within streambed sediments and lead to an increase in streambed hydraulic conductivity, which in turn will likely enhance hyporheic exchange (Song et al. 2007), whereas downward flow in streambeds on the other hand can reduce hydraulic conductivity (Rosenberry and Pitlick 2009). Nevertheless, one cannot comment definitively on the possible influence of these factors on the spatial distribution of streambed K_v and water fluxes in this study. Additional measurements beyond the scope of the current work would be needed to fully evaluate the importance of sedimentary structures, clogging processes, and hyporheic processes as possible controls on spatial variability of streambed K_v and water fluxes.

Conclusions

In this report, vertical water fluxes are estimated using vertical temperature profiles and the Darcian flux calculations at three

Table 5 Sediment grain-size distributions for the three test sites

Grain size	Site MB					Site AC					Site SC				
	E1	E2	C	D2	D1	E1	E2	C	D2	D1	E1	E2	C	D2	D1
Average value of cumulative percentage in weight (%)															
<2 mm	99.4	99.6	97.5	99.8	96.2	87.1	90.3	88.2	85.2	86.9	96.0	95.0	85.8	96.3	93.6
<0.075 mm (silt + clay)	1.6	1.0	7.9	4.6	40.9	4.0	26.9	1.2	4.1	6.3	6.5	10.6	12.6	4.8	17.4
Average median grain size															
d50(mm)	0.17	0.19	0.18	0.18	0.15	0.35	0.48	0.15	0.57	0.26	0.27	0.57	0.57	0.58	0.34

different stream morphologies (meander bend, anabranching channel, and straight channel) in the Beiluo River in January 2015. A total number of 65 measurements at three sites were analyzed.

Obvious discrepancies of water fluxes in direction and magnitude obtained by the two methods are observed at some test locations of each site. The discrepancies of directions are mainly related to the variations of head gradient and streambed temperature over time, also possibly attributed to shallow temperature cycling through shallow streambed sediments and heterogeneity in streambed K_v or even measurement difficulty in the pipes. At the 28 test locations, values of VHG-derived upward fluxes show greater variability than the values of temperature-derived upward fluxes. The discrepancies of magnitudes are mainly associated with the different nature of the two approaches (streambed hydraulic conductivity and thermal conductivity). The approach of using vertical temperature profiles tends to underestimate or overestimate VHG-derived upward fluxes at some test locations when the assumption of steady-state conditions is violated.

Despite these discrepancies, the results of the Kruskal-Wallis tests show no significant differences between the estimated upward fluxes based on vertical temperature profiles and Darcian flux calculations at each test site, showing that both approaches are applicable for estimating vertical water fluxes. Spatial variability of the upward fluxes based on vertical temperature profiles and the Darcian flux calculations also show a relatively good agreement, and are also relatively similar with spatial variability of K_v values or VHG values, indicating higher fluxes at certain locations with higher K_v values or higher VHG values and lower fluxes at certain locations with lower K_v values. Although there are not always statistically significant correlations between the upward fluxes and K_v or VHG, higher upward water fluxes are observed from the center of the channel towards the erosional bank at the MB site, near the erosional bank and in the center of channel at the AC site, and from the center of the channel towards the depositional bank at the SC site, where higher streambed K_v or higher VHG value are observed. Lower upward water fluxes are observed between the depositional bank and the center of the channel at the MB site and at the AC site, and near the erosional bank at the SC site, where lower streambed K_v are observed. Furthermore, the magnitude of vertical streambed water fluxes can vary spatially within scales of only a few meters apart; this difference also exists in the flux direction, especially for flux estimates based on the Darcian flux calculations. This significant spatial variability of flux patterns may be the combination of the regional-scale groundwater flow and local small-scale flow dynamics in the hyporheic zone that work together.

The stream morphology along the Beiluo River has had significant effect on erosional and depositional conditions, and streambed grain-size distribution, thereby affecting

streambed K_v and water fluxes. Significantly negative correlations between silt-clay content of the sediment and streambed K_v or vertical fluxes suggest that sediment grain size is one of major controlling factors of streambed K_v and water fluxes at the three test sites. This study only examined the influence of sediment grain size on streambed K_v and water fluxes, but the influence of other factors such as sedimentary structures, clogging processes, and hyporheic processes need to be resolved in future study.

Despite the existing discrepancies, the presented method focuses on spatial variability of the groundwater/surface-water interaction across the channel. Using vertical temperature profiles and the Darcian flux calculations in combination can provide a powerful tool for improving the understanding of the investigated hydrogeological conditions and enhance more accurate estimation of groundwater/surface-water connectivity in the Beiluo River. Especially, the use of vertical streambed temperature profiles can provide relatively acceptable vertical streambed water fluxes only by simple and fast temperature measurements; it is very appealing to researchers to have the convenient method for the first quantitative estimate of vertical streambed water fluxes before the large-scale investigation. Of course, determination of the streambed vertical hydraulic conductivity and VHGs at some test locations are also needed to confirm the direction and magnitude of vertical streambed water fluxes. In order to increase the level of certainty, the two methods in combination with other methods such as chemical and isotopic tracers will be useful in providing more accurate flux estimates.

Acknowledgements This study was supported by the National Natural Science Foundation of China (grant Nos. 51379175 51679200 and 51308457), Specialized Research Fund for the Doctoral Program of Higher Education (grant No. 20136101110001), Program for Key Science and Technology Innovation Team in Shaanxi Province (grant No. 2014KCT-27), The Hundred Talents Project of the Chinese Academy of Sciences (grant No. A315021406). We are especially grateful to the associate editor and three anonymous reviewers for their helpful suggestions, which improved the quality of the manuscript.

References

- Anderson MP (2005) Heat as a ground water tracer. *Ground Water* 43(6): 951–968. doi:10.1111/j.1745-6584.2005.00052.x
- Anibas C, Fleckenstein JH, Volze N, Buis K, Verhoeven R, Meire P, Batelaan O (2009) Transient or steady-state? Using vertical temperature profiles to quantify groundwater-surface water exchange. *Hydrological Processes* 23:2165–2177. doi:10.1002/hyp.7289
- Anibas C, Buis K, Verhoeven R, Meire P, Batelaan O (2011) A simple thermal mapping method for seasonal spatial patterns of groundwater-surface water interaction. *J Hydrol* 397:93–104. doi:10.1016/j.jhydrol.2010.11.036
- Arriaga MA, Leap DI (2004) Using solver to determine vertical groundwater velocities by temperature variations, Purdue University, Indiana, USA. *Hydrogeol J* 14:253–263. doi:10.1007/s10040-004-0381-x

- Bartsch S, Frei S, Ruidisch M, Shope CL, Peiffer S, Kim B, Fleckenstein JH (2014) River-aquifer exchange fluxes under monsoonal climate conditions. *J Hydrol* 509:601–614. doi:10.1016/j.jhydrol.2013.12.005
- Becker MW, Georgian T, Ambrose H, Siniscalchi J, Fredrick K (2004) Estimating flow and flux of groundwater discharge using water temperature and velocity. *J Hydrol* 296(1–4):221–233. doi:10.1016/j.jhydrol.2004.03.025
- Bencala KE, Gooseff MN, Kimball BA (2011) Rethinking hyporheic flow and transient storage to advance understanding of stream-catchment connections. *Water Resour Res* 47(3). doi:10.1029/2010WR010066
- Binley A, Ullah S, Heathwaite AL, Heppell C, Byrne P, Lansdown K, Trimmer M, Zhang H (2013) Revealing the spatial variability of water fluxes at the groundwater-surface water interface. *Water Resour Res* 49:3978–3992. doi:10.1002/wrcr.20214
- Birkel C, Soulsby C, Irvine DJ, Malcolm I, Lautz LK, Tetzlaff D (2016) Heat-based hyporheic flux calculations in heterogeneous salmon spawning gravels. *Aquat Sci* 78(2):203–213. doi:10.1007/s00027-015-0417-4
- Blaschke AP, Steiner KH, Schmalfluss R, Gutknecht D, Sengschmitt D (2003) Clogging processes in hyporheic interstices of an impounded river, the Danube at Vienna, Austria. *Int Rev Hydrobiol* 88:397–413
- Bredehoeft J, Papaopulos I (1965) Rates of vertical groundwater movement estimated from the earth's thermal profile. *Water Resour Res* 1: 325–328
- Brunke M, Gonser T (1997) The ecological significance of exchange processes between rivers and groundwater. *Freshw Biol* 37:1–33
- Bruno MC, Maiolini B, Carolli M, Silveri L (2009) Impact of hydropeaking on hyporheic invertebrates in an Alpine stream (Trentino, Italy). *Annal Limnol* 45:157–170
- Calver A (2001) Riverbed permeabilities: information from pooled data. *Groundwater* 39:546–553
- Cardenas MB, Wilson JL, Zlotnik VA (2004) Impact of heterogeneity, bed forms, and stream curvature on subchannel hyporheic exchange. *Water Resour Res* 40. doi:10.1029/2004wr003008
- Cey EE, Rudolph DL, Parkin GW, Aravena R (1998) Quantifying groundwater discharge to a small perennial stream in southern Ontario, Canada. *J Hydrol* 210:21–37. doi:10.1016/S0022-1694(98)00172-3
- Chapman SW, Parker BL, Cherry JA, Aravena R, Hunkeler D (2007) Groundwater-surface water interaction and its role on TCE groundwater plume attenuation. *J Contam Hydrol* 91:203–232
- Chen XH (2004) Streambed hydraulic conductivity for rivers in south-central Nebraska. *J Am Water Resour Assoc* 40:561–573
- Chen XH, Song JX, Cheng C, Wang DM, Lackey SO (2009) A new method for mapping variability in vertical seepage flux in streambeds. *Hydrogeol J* 17:519–525. doi:10.1007/s10040-008-0384-0
- Chen X, Dong W, Ou G, Wang Z, Liu C (2013) Gaining and losing stream reaches have opposite hydraulic conductivity distribution patterns. *Hydrol Earth Syst Sci* 17:2569–2579. doi:10.5194/hess-17-2569-2013
- Conant B (2004) Delineating and quantifying ground water discharge zones using streambed temperatures. *Groundwater* 42:243–257. doi:10.1111/j.1745-6584.2004.tb02671.x
- Constantz J, Stewart AE, Niswonger R, Sarma L (2002) Analysis of temperature profiles for investigating stream losses beneath ephemeral channels. *Water Resour Res*. 38:52-51–52-13. doi:10.1029/2001wr001221
- Dujardin J, Anibas C, Bronders J, Jamin P, Hamonts K, Dejonghe W, Brouyère S, Batelaan O (2014) Combining flux estimation techniques to improve characterization of groundwater-surface-water interaction in the Zenne River, Belgium. *Hydrogeol J* 22:1657–1668. doi:10.1007/s10040-014-1159-4
- Duque C, Müller S, Sebok E, Haider K, Engesgaard P (2015) Estimating groundwater discharge to surface waters using heat as a tracer in low flux environments: the role of thermal conductivity. *Hydrol Processes*. doi:10.1002/hyp.10568
- Essaid HI, Zamora CM, McCarthy KA, Vogel JR, Wilson JT (2008) Using heat to characterize streambed water flux variability in four stream reaches. *J Environ Qual* 37:1010–1023. doi:10.2134/jeq2006.0448
- Fleckenstein J, Anderson M, Fogg G, Mount J (2004) Managing surface water-groundwater to restore fall flows in the Consummes River. *J Water Res Pl-ASCE* 130(4):301–310. doi:10.1016/(ASCE)0733-9496(2004)130:4(301)
- Flewelling SA, Herman JS, Hornberger GM, Mills AL (2012) Travel time controls the magnitude of nitrate discharge in groundwater bypassing the riparian zone to a stream on Virginia's coastal plain. *Hydrol Process* 26:1242–1253. doi:10.1002/hyp.8219
- Freeze RA, Cherry J (1979) *Groundwater*. Prentice-Hall, Englewood Cliffs, NJ, 604 pp
- Frei S, Lischeid G, Fleckenstein JH (2010) Effects of micro-topography on surface-subsurface exchange and runoff generation in a virtual riparian wetland: a modeling study. *Adv Water Res* 33:1388–1401. doi:10.1016/j.advwatres.2010.07.006
- Gariglio FP, Tonina D, Luce CH (2013) Spatiotemporal variability of hyporheic exchange through a pool-riffle-pool sequence. *Water Resour Res* 49:7185–7204. doi:10.1002/wrcr.20419
- Genereux DP, Leahy S, Mitasova H, Kennedy CD, Corbett DR (2008) Spatial and temporal variability of streambed hydraulic conductivity in West Bear Creek, North Carolina, USA. *J Hydrol* 358:332–353. doi:10.1016/j.jhydrol.2008.06.017
- Harvey JW, Bencala KE (1993) The effect of streambed topography on surface-subsurface water exchange in mountain catchments. *Water Resour Res* 29:89–98
- Helsel DR, Hirsch RM (1992) *Statistical methods in water resources*. Elsevier, Amsterdam, The Netherlands
- Hester ET, Gooseff MN (2010) Moving beyond the banks: hyporheic restoration is fundamental to restoring ecological services and functions of streams. *Environ Sci Technol* 44:1521–1525. doi:10.1021/es902988n
- Hvorslev MJ (1951) Time lag and soil permeability in ground-water observations. *US Army Bull* 36, Waterways Experiment Station, US Corps of Eng., Vicksburg, MI
- Hyun Y, Kim H, Lee S-S, Lee K-K (2011) Characterizing streambed water fluxes using temperature and head data on multiple spatial scales in Munsan stream, South Korea. *J Hydrol* 402:377–387
- Irvine DJ, Cranswick RH, Simmons CT, Shanfield MA, Lautz LK (2015) The effect of streambed heterogeneity on groundwater-surface water exchange fluxes inferred from temperature time series. *Water Resour Res* 51(1):198–212. doi:10.1002/2014WR015769
- Jiang WW, Song JX, Zhang JL, Wang YY, Zhang N, Zhang XH, Long YQ, Li JX, Yang XG (2015) Spatial variability of streambed vertical hydraulic conductivity and its relation to distinctive stream morphologies in the Beiluo River, Shaanxi Province, China. *Hydrogeol J* 23: 1617–1626. doi:10.1007/s10040-015-1288-4
- Kalbus E, Reinstorf F, Schirmer M (2006) Measuring methods for groundwater-surface water interactions: a review. *Hydrol Earth Syst Sci* 10:873–887. doi:10.5194/hess-10-873-2006
- Kasahara T, Wondzell SM (2003) Geomorphic controls on hyporheic exchange flow in mountain streams. *Water Resour Res* 39. doi:10.1029/2002WR001386
- Käser DH, Binley A, Heathwaite AL, Krause S (2009) Spatio-temporal variations of hyporheic flow in a riffle-step-pool sequence. *Hydrol Process* 23(15):2138–2149. doi:10.1002/hyp.7317
- Kennedy CD, Genereux DP, Corbett DR, Mitasova H (2009) Spatial and temporal dynamics of coupled groundwater and nitrogen fluxes through a streambed in an agricultural watershed. *Water Resour Res* 45. doi:10.1029/2008wr007397
- Kennedy CD, Murdoch LC, Genereux DP, Corbett DR, Stone K, Pham P, Mitasova H (2010) Comparison of Darcian flux calculations and

- seepage meter measurements in a sandy streambed in North Carolina, United States. *Water Resour Res* 46. doi:10.1029/2009wr008342
- Leek R, Wu JQ, Wang L, Hanrahan TP, Barber ME, Qiu HX (2009) Heterogeneous characteristics of streambed saturated hydraulic conductivity of the Touchet River, south eastern Washington, USA. *Hydrol Process* 23:1236–1246
- Lewandowski J, Putschew A, Schwesig D, Neumann C, Radke M (2011) Fate of organic micropollutants in the hyporheic zone of a eutrophic lowland stream: results of a preliminary field study. *Sci Total Environ* 409:1824–1835
- Loheide SP, Gorelick SM (2006) Quantifying stream–aquifer interactions through the analysis of remotely sensed thermographic profiles and in situ temperature histories. *Environ Sci Technol* 40(10):3336–3341. doi:10.1021/es0522074
- Malard F, Tockner K, Dole-Olivier MJ, Ward J (2002) A landscape perspective of surface–subsurface hydrological exchanges in river corridors. *Freshw Biol* 47:621–640
- Malcolm IA, Youngson AF, Greig S, Soulsby C (2008) Hyporheic influences on spawning success. In: Sear D, DeVries P (eds) *Salmon spawning habitat in rivers: physical controls, biological responses and approaches to remediation*. American Fisheries Society, Symposium 65, Bethesda, pp 225–248
- Merwade VM, Maidment DR, Goff JA (2006) Anisotropic considerations while interpolating river channel bathymetry. *J Hydrol* 331(3):731–741. doi:10.1016/j.jhydrol.2006.06.018
- Packman AI, Marion A, Zaramella M, Chen C, Gaillard JF, Keane DT (2006) Development of layered sediment structure and its effects on pore water transport and hyporheic exchange. *Water Air Soil Pollut Focus* 6(5–6):433–442. doi:10.1007/s11267-006-9057-y
- Rau GC, Andersen MS, McCallum AM, Acworth RI (2010) Analytical methods that use natural heat as a tracer to quantify surface water–groundwater exchange, evaluated using field temperature records. *Hydrogeol J* 18:1093–1110. doi:10.1007/s10040-010-0586-0
- Roque AJ, Didier G (2006) Calculating hydraulic conductivity of fine-grained soils to leachates using linear expressions. *Eng Geol* 85(1):147–157
- Rosenberry DO, Pitlick J (2009) Effects of sediment transport and seepage direction on hydraulic properties at the sediment–water interface of hyporheic settings. *J Hydrol* 373:377–391. doi:10.1016/j.jhydrol.2009.04.030
- Saleem Z (1970) A computer method for pumping-test analysis. *Ground Water* 8:21–24
- Savant SA, Reible DD, Thibodeaux LJ (1987) Convective transport within stable river sediments. *Water Resour Res* 23:1763–1768
- Schmidt C, Bayer-Raich M, Schirmer M (2006) Characterization of spatial heterogeneity of groundwater–streamwater interactions using multiple depth streambed temperature measurements at the reach scale. *Hydrol Earth Syst Sci* 10:849–859
- Schmidt C, Conant B Jr, Bayer-Raich M, Schirmer M (2007) Evaluation and field-scale application of an analytical method to quantify groundwater discharge using mapped streambed temperatures. *J Hydrol* 347:292–307. doi:10.1016/j.jhydrol.2007.08.022
- Schornberg C, Schmidt C, Kalbus E, Fleckenstein JH (2010) Simulating the effects of geologic heterogeneity and transient boundary conditions on streambed temperatures: implications for temperature-based water flux calculations. *Adv Water Resour* 33(11):1309–1319. doi:10.1016/j.advwatres.2010.04.007
- Sebok E, Duque C, Engesgaard P, Boegh E (2015) Spatial variability in streambed hydraulic conductivity of contrasting stream morphologies: channel bend and straight channel. *Hydrol Process* 29:458–472. doi:10.1002/hyp.10170
- Silliman SE, Ramirez J, McCabe RL (1995) Quantifying downflow through creek sediments using temperature time series: one-dimensional solution incorporating measured surface temperature. *J Hydrol* 167:99–119
- Smith JWN (2005) *Groundwater–surface water interactions in the hyporheic zone*. Environment Agency–Science Report SC030155/SR1, Bristol
- Song JX, Chen XH, Cheng C, Summerside S, Wen FJ (2007) Effects of hyporheic processes on streambed vertical hydraulic conductivity in three rivers of Nebraska. *Geophys Res Lett* 34, L07409. doi:10.1029/2007gl029254
- Song JX, Jiang WW, Xu SF, Zhang GT, Wang LP, Wen M, Zhang B, Wang YY, Long YQ (2016) Heterogeneity of hydraulic conductivity and Darcian flux in the submerged streambed and adjacent exposed stream bank of the Beiluo River, northwest China. *Hydrol J*: 1–14. doi:10.1007/s10040-016-1449-0
- Stallman R (1965) Steady one-dimensional fluid flow in a semi-infinite porous medium with sinusoidal surface temperature. *J Geophys Res* 70:2821–2827
- Storey RG, Howard KWF, Williams DD (2003) Factors controlling riffle-scale hyporheic exchange flows and their seasonal changes in a gaining stream: a three-dimensional groundwater flow model. *Water Resour Res* 39. doi:10.1029/2002wr001367
- Suzuki S (1960) Percolation measurements based on heat flow through soil with special reference to paddy fields. *J Geophys Res* 65:2883–2885
- Swanson TE, Bayani Cardenas M (2010) Diel heat transport within the hyporheic zone of a pool–riffle–pool sequence of a losing stream and evaluation of models for fluid flux estimation using heat. *Limnol Oceanogr* 55(4):1741–1754. doi:10.4319/lo.2010.55.4.1741
- Taniguchi M, Shimada J, Tanaka T, Kayane I, Sakura Y, Shimano Y, Dapaah-Siakwan S, Kawashima S (1999) Disturbances of temperature–depth profiles due to surface climate change and subsurface water flow: 1. an effect of linear increase in surface temperature caused by global warming and urbanization in the Tokyo Metropolitan Area, Japan. *Water Resour Res* 35:1507–1517. doi:10.1029/1999wr900009
- Team RC (2016) R: a language and environment for statistical computing, Vienna, Austria. <https://www.r-project.org>. Accessed 20 April 2016
- Vandersteen G, Schneidewind U, Anibas C, Schmidt C, Seuntjens P, Batelaan O (2015) Determining groundwater–surface water exchange from temperature–time series: combining a local polynomial method with a maximum likelihood estimator. *Water Resour Res* 51: 922–939. doi:10.1002/2014wr015994
- Vaux W (1968) Intragravel flow and interchange of water in a streambed. *US Fish Wildl Serv Fish Bull* 66:479–489
- Winter TC (1998) *Ground water and surface water: a single resource*. Diane, Darby, PA